Optimization Design and Performance Analysis of Bearingless Flux Switching Permanent Magnet Motor with Multi-tooth Structure

Ying Xu, and Huangqiu Zhu
School of Electrical and Information Engineering, Jiangsu University, Zhenjiang 212013, Jiangsu, China

26th International Conference on Magnet Technology
Poster ID :Tue-Af-Po2.20-10(Poster Session)

Background

The traditional bearingless motor places the PM on the rotor, which results in the low power density, poor speed regulation ability and weak mechanical strength of the motor. Therefore, more and more attention has been paid to the structure of placing PM on the stator in recent years. In stator PM bearingless motor, the bearingless flux switching permanent magnet (BFSPM) motor has attracted more interests due to its high torque density, high power density, large torque output ability and strong loading capacity.

Motor Topology

Configuration

The 2D model of six-phase, 24-slot/10-pole multi-tooth BFSPM motor is composed of stator, rotor, auxiliary slots, six-phase non-overlapping centralized stator windings and alternating magnetized permanent magnets.

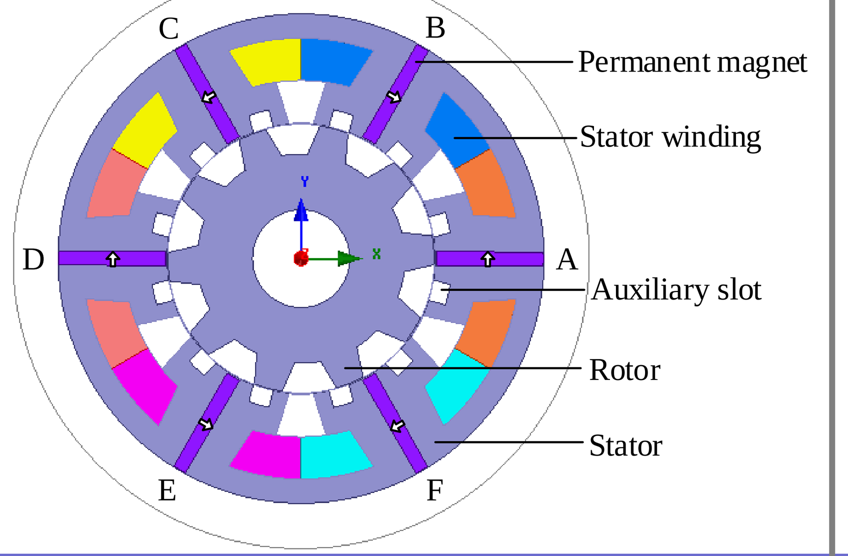

Working Principle

When the suspension force winding current is introduced, the balance of the air gap magnetic field produced by the torque windings will be broken. According to the Maxwell tensor method, the radial suspension force will be produced.

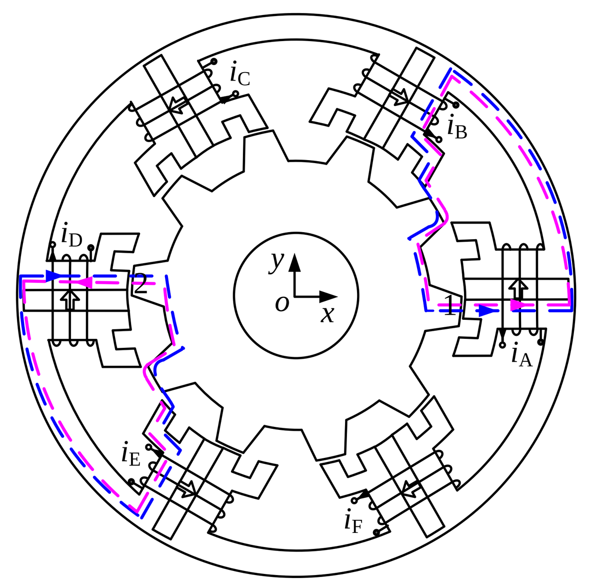

Parameter Design

The magnetic conductivity between stator teeth and rotor pole are P_{sr1}, P_{sr2}, P_{sr3}, P_{sr4}, P_{sr5} and P_{sr6}. Ignoring the high order harmonics, the expressions of the magnetic conductivity in each part are obtained. Assuming that the current is certain, the motor works in BLAC mode, the magneto-resistive torque can be ignored. If the stator pole number N_s and the stator tooth width are constant, the value of the coefficient k_a is only related to N_r. The torque reaches the maximum when the rotor pole number N_r is 21. Therefore, the pole number ratio of stator and rotor is 24/21.

$$\begin{cases} P_{sr1}=\sum_{i=1}^{2}\left(P_0+P_1\cos\left(N_r\theta_{0sr}+P_r\left(\frac{2\pi}{N_s}-(2i-1)\theta_1\right)\right)\right) \\ P_{sr2}=tP_0+tP_1\cos\left(N_r\theta_{0sr}+N_r\frac{\pi}{N_s}\right) \\ P_{sr3}=\sum_{i=1}^{2}\left(P_0+P_1\cos\left(N_r\theta_{0sr}+(2i-1)N_r\theta_1\right)\right) \\ P_{sr4}=\sum_{i=1}^{2}\left(P_0+P_1\cos\left(N_r\theta_{0sr}-(2i-1)N_r\theta_1\right)\right) \\ P_{sr5}=tP_0+tP_1\cos\left(N_r\theta_{0sr}-N_r\frac{\pi}{N_s}\right) \\ P_{sr6}=\sum_{i=1}^{2}\left(P_0+P_1\cos\left(N_r\theta_{0sr}-N_r\left(\frac{2\pi}{N_s}-(2i-1)\theta_1\right)\right)\right) \end{cases}$$

$$\theta_{0sr}=\pi/2N_r$$

$$T_e=\frac{m}{2}N_r\varphi_m I_q\propto N_r\left(\frac{P_{sr4}}{P_{sr4}+P_{sr5}+P_{sr6}}-\frac{P_{sr3}}{P_{sr1}+P_{sr2}+P_{sr3}}\right)=N_r k_a$$

$$k_a=\sum_{i=0}^{1}\frac{2+(-1)^i\sum_{j=1}^{2}\sin(2j-1)N_r\theta_1}{(4+t)+(-1)^i\sum_{j=1}^{2}\left(\sin(2j-1)N_r\theta_1+\sin\left(\frac{2\pi N_r}{N_s}-(2j-1)N_r\theta_1\right)\right)+(-1)^i t\sin\left(\frac{\pi N_r}{N_s}\right)}$$

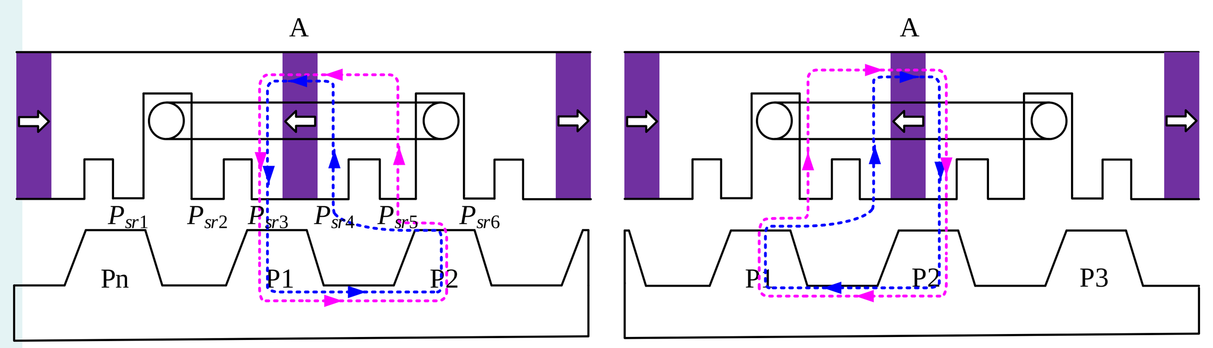

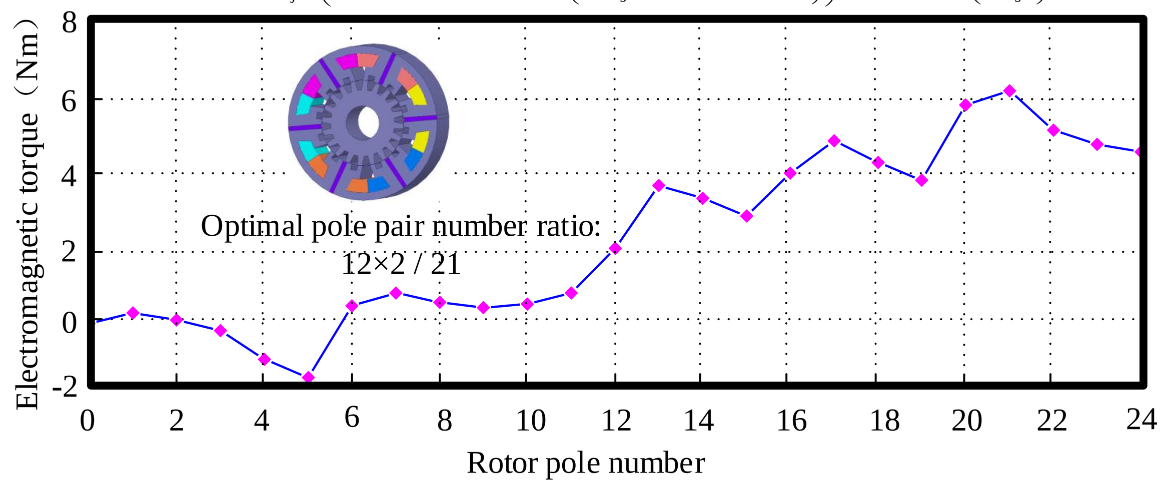

Symbol	Quantity	Value
P	Phase number	6
N_s	Stator pole number	12×2
N_r	Rotor pole number	21
d_{so}	Stator outer diameter	125mm
d_{si}	Stator inner diameter	68.75mm
g	Air gap length	0.5mm
d_{ri}	Rotor inner diameter	22mm
B_r	Magnet remanence	1.2T
l_a	Motor stack length	60mm
n	Rated speed	3000r/min
N	Number of turns	100
H_c	Coercive force	-890kA/m
A_s	Effective value of linear load	26.1kA/mm
P_N	Rated power	2kW
h_s	Stator tooth width	3.92mm
h_{pm}	Permanent magnet thickness	3.92mm
h_r	Rotor tooth width	7.54mm
h_{slot}	Stator slot width	3.92mm
l_{slot}	Stator slot height	3.92mm
k_{sio}	Split ratio	0.55
l_{pm}	Permanent magnet length	27.5mm

Finite Element Analysis

No-load characteristic

The simulations are designed to analyze the magnetic flux density, no-load back-EMF, the no load PM flux linkage and the harmonic of the motor. The 2D model, magnetic field distribution, grid division, magnetic density cloud and air gap magnetic density of the multi-tooth type BFSPM motor are shown.

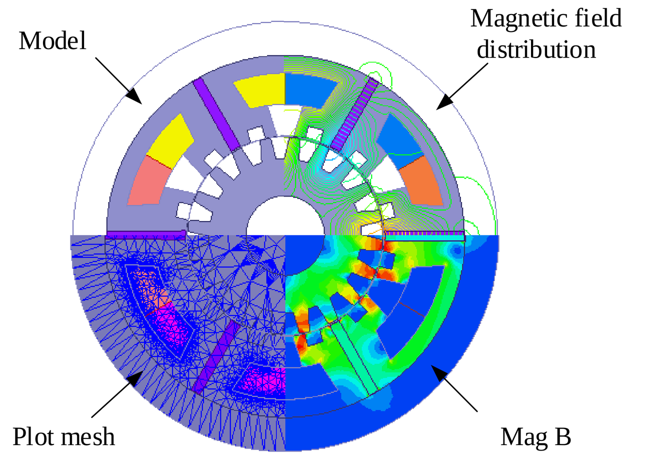

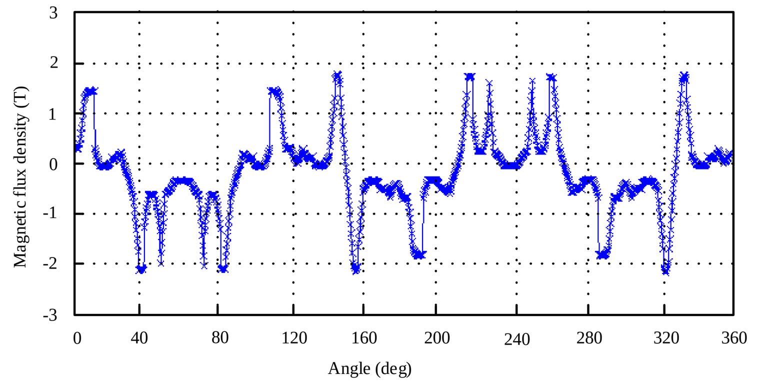

After Fourier analysis and calculation in , it can be seen that the harmonic distortion rates of no-load back EMF and no-load PM flux linkage are 15.7% and 8.7%, respectively, which indicates that the no-load back EMF waveform of the motor has good sinusoidal degree.

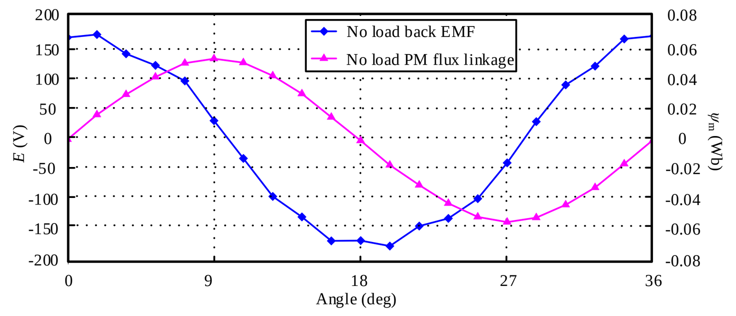

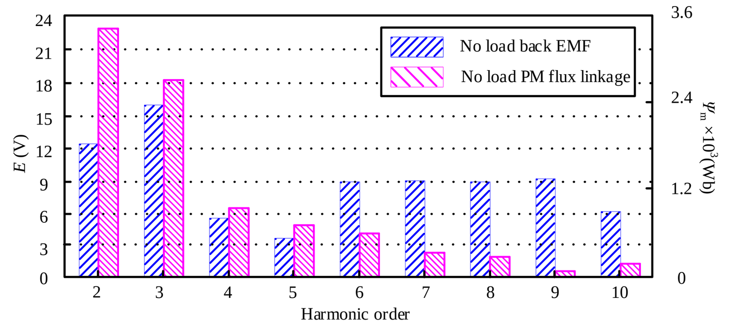

Cogging torque

It can be seen that the cogging torque peak value of traditional BFSPM motor is 2.8 N·m, and that of the multi-tooth is 1.2 N·m. The value of cogging torque is reduced by about 57.1%.

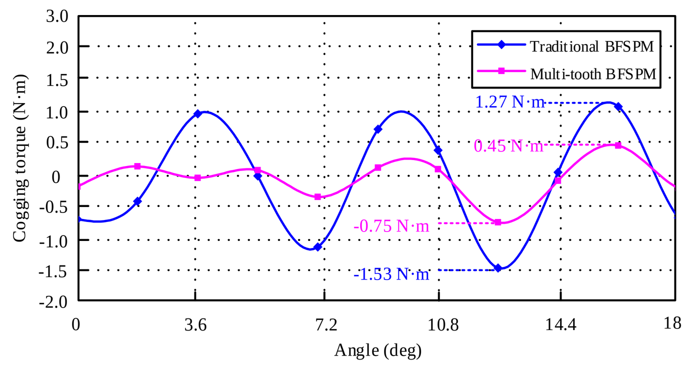

Electromagnetic torque

The average torque of multi-tooth motor is 6.90N·m, which is almost the same as that of the traditional motor, it means that the power density will not decrease. Meanwhile, the torque ripple ratio value of the above two motors are 23.96% and 11.38% , respectively.

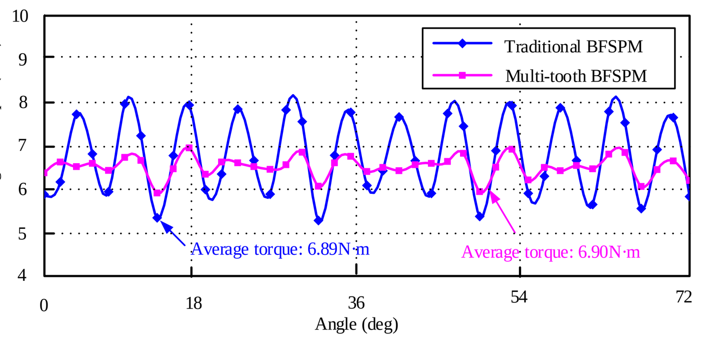

Radial suspension force

The average suspension force of multi-tooth BFSPM motor is 240.93 N, which is higher than that of traditional BFSPM motor. The suspension force ripple ratio value of them are 18.35% and 17.28%, respectively.

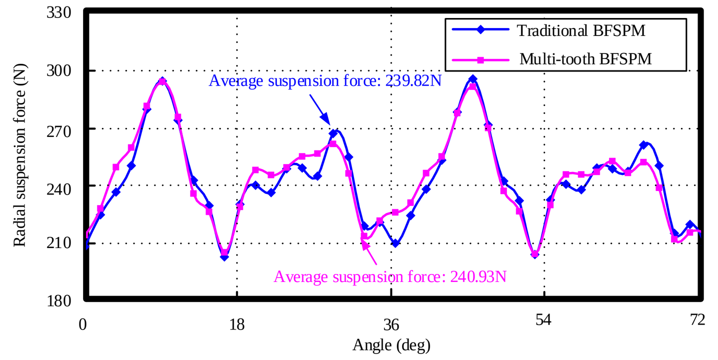

Conclusion

In this paper, a six-phase multi-tooth BFSPM motor is designed to improve the performance of the motor. The basic structure and operation principle are introduced, and the optimal pole number ratio of stator and rotor is calculated by the magnetic conductivity formula. The key dimension parameters of the motor are designed. The no-load characteristic, cogging torque, electromagnetic torque and radial suspension force of the motor are analyzed by the FEA. Compared with a traditional BFSPM motor, it has been shown that: 1) the number of PMs used in the proposed motor is only half of that used in the traditional BFSPM motor. 2) it exhibits a higher torque density at relatively low currents, but as the magnetic circuit becomes saturates more quickly as the current is increased. 3) the proposed BFSPM motor can effectively reduce the torque ripple and improve the suspension performance.